www.springer.com/41230
https://doi.org/10.1007/s41230-025-4240-9

Vat photopolymerization 3D printing of ceramic cores: Advances, challenges, and prospects

Xiang Li, *Hai-jun Su, Dong Dong, Hao Jiang, Ya-wen Ma, Zhong-lin Shen, Yi-nuo Guo, Yun Zhang, Zhuo Zhang, and Min Guo

State Key Laboratory of Solidification Processing, Northwestern Polytechnical University, Xi'an 710072, China

Abstract: To meet the evolving demands of aeroengine development, the structural and performance requirements for ceramic cores have become increasingly stringent. Vat photopolymerization 3D printing, owing to its moldless, flexible manufacturing, and other advantages, demonstrates significant potential in the preparation of ceramic cores with intricate structures. However, its practical application still faces multiple challenges, including layered structures and property anisotropy, defects such as cracks and collapse during printing and sintering, forming inaccuracies, and difficulties in controlling surface roughness. Recent advances have focused on optimizing slurry formulation and rheology, improving curing behavior, introducing auxiliary powders and additives, tailoring forming parameters, and optimizing the sintering process. Nevertheless, effectively suppressing lamellar defects, achieving superior dimensional accuracy, and maintaining high surface quality in complex structures remain the core scientific and technical issues to be solved. Future research should concentrate on refining curing mechanisms, advancing powder design and organic system optimization, and regulating the coupled processes of forming, debinding, and sintering to accelerate the application of VPP 3D printed ceramic cores in aerospace manufacturing.

Keywords: vat photopolymerization; ceramic cores; layered structures; forming accuracy

CLC numbers: TG221$^+$.2 **Document code:** A **Article ID:** 1672-6421(2025)05-493-14

1 Introduction

Ceramic cores are typically utilized for forming the internal cavities of complex components in investment casting[1, 2]. The ceramic cores used for aircraft engine turbine blades represent the highest level of preparation for ceramic cores due to their structural complexity and performance requirements[3, 4]. Meanwhile, the pursuit of an improved thrust-to-weight ratio in aerospace engines requires ceramic cores with even more intricate structures and higher performance standards[5, 6].

The traditional preparation method for ceramic cores is mainly injection molding, which relies on molds and involves a lengthy process cycle[7]. Additive manufacturing technology, due to its moldless and flexible manufacturing advantages, possesses advantages in the field of preparing complex structural components[8]. Since Halloran et al.[9-11] developed ceramic stereolithography (SLA) technology in the 1990s, various ceramic additive manufacturing technologies with different principles have been developed, such as digital light processing (DLP)[12], liquid crystal display (LCD)-based 3D printing[13, 14], inkjet printing (IJP)[15, 16], direct ink writing (DIW)[17, 18], binder jetting (BJ)[19, 20], selective laser sintering (SLS)[21, 22], selective laser melting (SLM)[23, 24], and so on. Among them, SLA, DLP, and LCD are referred to as vat photopolymerization (VPP) 3D printing technology[25]. Compared to other ceramic additive manufacturing technologies, as shown in Table 1, VPP ceramic 3D printing demonstrates significant potential for fabricating the ceramic cores due to its high surface quality and high printing accuracy (~μm)[26, 27].

***Hai-jun Su**

Male, born in 1981, Ph. D., Professor. His research interests primarily focus on the theories and technologies of advanced directional solidification and additive manufacturing of various materials, including superalloys, high entropy alloys, ultra high-temperature composite ceramics, bioceramics, perovskite solar cells, and structural functional integrated composites. To date, he has led over 30 major national-level projects and published more than 200 papers in top-tier journals, including *Nano Energy*, *Advanced Functional Materials*, *Nano Letters*, and *Composites*. He holds more than 60 granted China's invention patents and 3 US patents. He was also granted with many awards & honors including the First and Second Prizes of Shaanxi Provincial Science & Technology Awards, the Second Prize of China Communications & Transportation Association Science & Technology Award, the First Prize of Shaanxi Metallurgical Science & Technology Award, the National Excellent Youth Science & Technology Award in Nonferrous Metals, among others.

E-mail: shjnpu@nwpu.edu.cn

Received: 2024-11-04; Revised: 2024-11-25; Accepted: 2024-12-02

Table 1: Main process parameters of SLA 3D printed alumina ceramic cores[28-34]

Additive manufacturing technology	Ceramic core matrix	Resolution	Surface quality
VPP	Alumina, silica, etc.	μm	Excellent
DIW	Calcia, etc.	μm–mm	Low
SLS	Silica, mullite, etc.	μm–mm	Low
BJ	Calcium carbonate, alumina, etc.	μm–mm	Medium

However, there are significant challenges in applying VPP 3D printing technology to fabricate ceramic cores with complex structures[35, 36]. These challenges primarily arise from the conflict between the process requirements of VPP 3D printing and the comprehensive performance requirements of ceramic cores.

VPP 3D printing necessitates ceramic slurries with low viscosity (typically≤5 Pa·s) and high solid loading[37], and the VPP printing process pursues higher curing depth, good interlayer bonding, and minimal light scattering to ensure forming accuracy. The debinding and sintering processes are crucial to ensure that there is no cracking or deformation in the final product. Further complicating matters are the interactions among the slurry preparation, debinding, and sintering processes. These underlying processes and mechanism need to be studied in depth.

In addition, the structural and performance requirements for ceramic cores are very stringent[1, 6, 38]. Currently, there are mainly two types of ceramic core matrices, alumina and silica, that applied in investment casting of aircraft engine turbine blades[39]. Silica-based ceramic cores employ fused quartz as the matrix, with sintering aids like alumina and zirconia incorporated. Conversely, alumina-based ceramic cores utilize alumina as the matrix, incorporating sintering aids such as silica, zirconia, and yttria. The comprehensive performance requirements for ceramic cores include suitable flexural strength (in both room and high temperature environments), certain porosity, low surface roughness, and excellent high-temperature creep resistance, among others[40]. Moreover, these properties are mutually constrained.

In order to achieve qualified VPP 3D printed ceramic cores, numerous researchers have undertaken targeted optimizations of the VPP 3D printing processes, including mold structure optimization, composition design, high-performance slurry preparation, and improvement of the printing, debinding, and sintering processes[35, 41]. This study summarizes the key issues in VPP 3D printing ceramic cores, including layered structures and anisotropy, defects suppression, optimization of forming accuracy and surface quality. By analyzing the underlying mechanisms and current mitigation strategies, this work aims to provide a comprehensive reference for process control, and quality assurance in ceramic additive manufacturing.

2 Layered structure and anisotropy

VPP 3D printing technology prepares complex structural parts through discrete and then stacked methods[25]. However, this stacking method results in a layered structure within the green body. Meanwhile, the properties of sintered ceramic cores exhibit anisotropy. This section summarizes the factors contributing to the layered structures and the anisotropic properties observed in VPP 3D printed ceramic cores.

2.1 Generation of layered structures

Ceramic fabrication processes are often characterized by a cumulative nature, wherein defects introduced in early stages cannot be fully mitigated by subsequent processing steps. For instance, friction among ceramic powders during traditional dry pressing can cause uneven powder accumulation[42]. This unevenness in the microstructure persists after the sintering process, ultimately influencing the properties of the ceramic parts. VPP 3D printing exhibits similar characteristics. The layer-by-layer stacking process in VPP 3D printing inherently leads to the formation of layered structures, which in turn affects the final properties of ceramic cores. Exploring the fundamental reasons and influencing factors causing the formation of layered structures is of great significance for regulating the microstructure and properties of ceramic cores.

Powder settling in ceramic slurry is a possible cause for the formation of layered structures. Zhao et al.[43] suggested that the ceramic powders in slurry will settle within a short period, creating gaps between layers during the printing process, as shown in Figs. 1(a) to (d). They evidenced this conjecture by yellowing phenomenon during the debinding stage. Certainly, settlement is a contributing factor. But different settlement rates of powders, combined with variations in slurry dispersion stability, can lead to the formation of distinct interlayer gaps.

Printing process has an important influence on the generation of layered structures. Li et al.[44] believed that the interaction between the scraper and the slurry during the printing process significantly affected the layered structure, as shown in Figs. 1(a1) to (e1). By simulating the slurry flow during scraper movement, it was found that smaller particles tended to concentrate on the top and bottom surfaces of each printed layer, while larger particles accumulated in the middle. As the sintering temperature increased, the pores among particles migrated towards the interfaces between the layers and coalesced to form larger pores at these interfaces. Li et al.[45] also simulated the effect of layer thickness on the formation of layered structures and found that the layer thickness was related to the movement state of the slurry. The simulation results indicated that turbulence and the displacement of the maximum-velocity zone, as clearly depicted in Figs. 1(a2) to (e2), exerted a substantial influence on the redistribution of ceramic particles with diverse sizes. This influence was particularly pronounced when the spreading thickness falled within the range of 100–200 μm, ultimately leading to the formation of a layered structure.

Discontinuity in curing behavior is another significant factor contributing to the formation of layered structures[46]. The curing degree of ceramic slurry follows a gradient

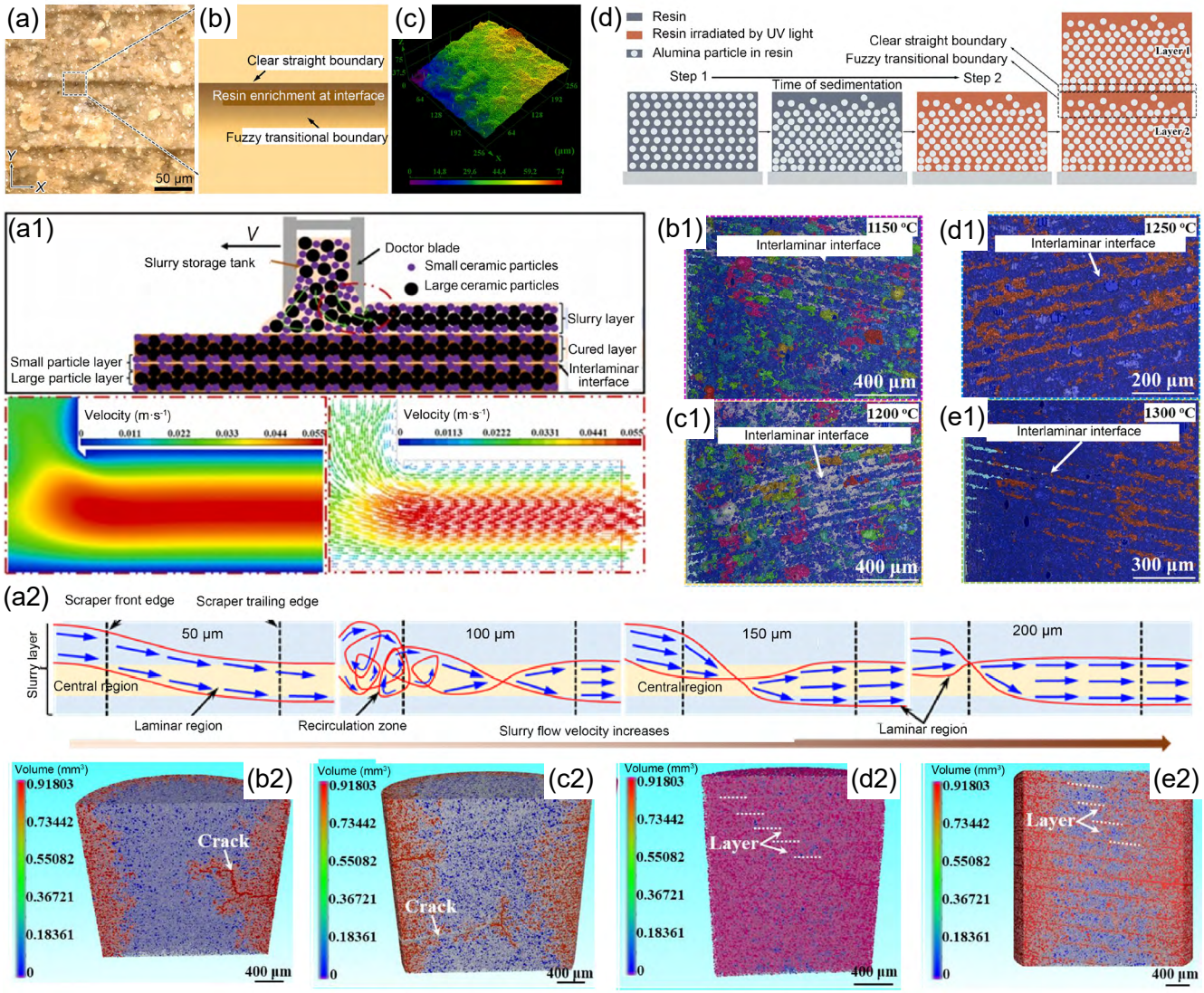

Fig. 1: Fracture surface of the brown body (a), and corresponding layered structure analysis (b) and three-dimensional surface image (c), as well as forming schematic diagram of layered structure (d)[43]: (a1) slurry flow simulation of ceramic core in the spreading process; (b1–e1) micro-nano CT results of ceramic core samples sintered at different temperatures of 1,150 °C (b1), 1,200 °C (c1), 1,250 °C (d1), and 1,300 °C (e1), respectively [44]. (a2) flow velocity of slurry with different spreading thicknesses; (b2–e2) micro/nano CT results with different print layer thicknesses of 50 μm (b2), 100 μm (c2), 150 μm (d2), and 200 μm (e2), respectively[45]

distribution along the curing direction, with the highest curing degree observed near the slurry surface where the light source is incident[47]. As the light source penetrates deeper into the slurry, the curing degree gradually decreases. Furthermore, the connection between layers relies on the curing of the previous layer by the subsequent one, which is one of the important reasons for the formation of layered structures. Factors that influence the curing process will also affect the generation of layered structures[48]. Li et al.[49] investigated the impact of curing depth on layered structures, as shown in Fig. 2. Their findings revealed that a lower curing depth is insufficient to guarantee robust interlayer connections, leading to noticeable layer separation. As the curing depth increases, the incident light can enhance the connection between the next layer and the current layer.

2.2 Performance anisotropy and controlling

Layered structures of VPP 3D printed ceramic cores are manifestations of anisotropic microstructure, and in most cases, the layered structure will be retained in the sintered sample and exhibit performance anisotropy. Niu et al.[50] optimized the anisotropy of silica-based ceramic cores by adding alumina powder. In ceramic cores without alumina powder, a multilayer structure with obvious interlayer gaps was observed in the horizontal printing direction, which was related to particle deposition during the printing process. When the alumina content reached 6wt.%, the microstructure became more uniform due to enhanced particle rearrangement between different layers. Li et al.[51] printed silica-based ceramic cores with different directions and controlled the anisotropy of the microstructure and properties using aluminum powder, as illustrated in Figs. 3(a1–e1). The optimized ceramic cores exhibited high-temperature strengths of 16.6 MPa and 16.1 MPa in different printing directions.

In subsequent research, Li et al.[52] used metallic silicon

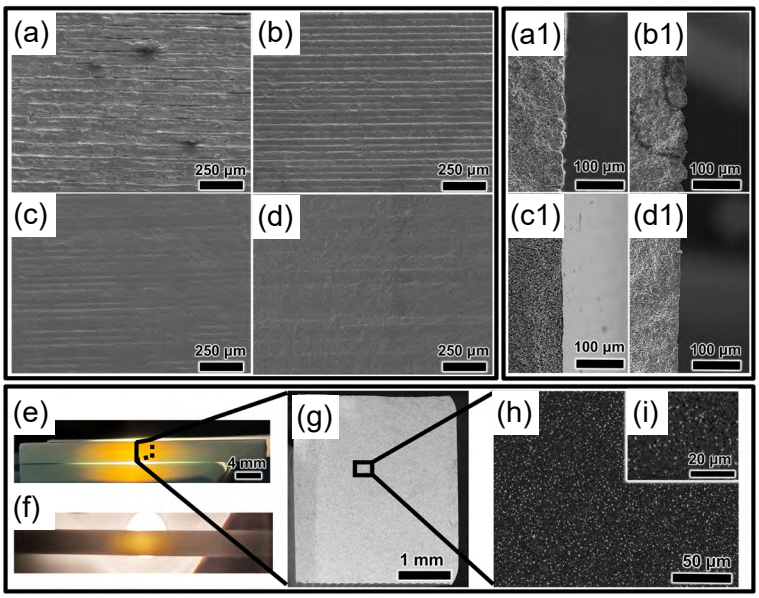

Fig. 2: Microstructures of sintered ceramic core samples with different curing depths: (a) 80 μm; (b) 100 μm; (c) 150 μm; (d) 200 μm; morphologies of samples with different curing depths: (a1) 80 μm; (b1) 100 μm; (c1) 150 μm; (d1) 200 μm; and sintered ceramic core sample with a curing depth of 150 μm: (e–f) different surfaces; (g–i) corresponding microstructure and local magnified image[49]

powder to regulate the interlayer structure in silica-based ceramic core fabricated by VPP 3D printing and observed that the volume expansion resulting from the conversion of metallic silicon to silica during sintering can partially fill the interlayer gaps and inhibit shrinkage rate.

Fan et al.[53] investigated the impact of different particle sizes of fused quartz on the mechanical properties anisotropy of VPP 3D printed ceramic cores, as shown in Figs. 3(a2–e2). The results indicated that the finer powder in the slurry had strong dispersibility and promoted the rearrangement of interlayer particles during the sintering process. As the particle size decreased from 35 μm to 5 μm, the ratio of vertical strength to horizontal strength (σ_V/σ_H) increased from 0.48 to 0.86, indicating enhanced mechanical uniformity.

The suppression of mechanical anisotropy mainly focuses on powder design, which can be divided into two parts: on the one hand, promoting particle rearrangement by increasing the sintering activity of the powder; on the other hand, compensating for interlayer gaps through additives[50–53]. These methods provide insights into the formation mechanisms of layered structures. However, the underlying causes remain incompletely understood, and more importantly, effective strategies for suppressing such structures require further development.

3 Defects of 3D printed ceramic cores

Layered structure is a prominent microstructural feature of VPP 3D printed ceramic cores[54], and poor control of the layered structure can easily lead to significant defects in VPP 3D printed ceramic cores. Furthermore, ceramic cores are characterized by their intricate structure, which makes their fabrication a challenging endeavor. Improper processes employed during printing, debinding, and sintering stages can equally trigger the emergence of cracks, surface defects, and even lead to complete formation failures.

An et al.[55, 56] conducted research on VPP 3D printed silica-based ceramic cores and found that cracks in these cores could be divided into interlayer cracks and intralayer cracks, as shown in Figs. 4(a) and (b). Intralayer cracking primarily arose from thermal and shrinkage stresses during sintering. Relatively uneven curing in the interlayer regions caused weak interlayer bonding, which facilitated crack initiation and propagation. Sepecifically, the number of cracks increased with the sintering temperatures. Furthermore, the impact of different printing directions on crack formation in silica-based ceramic cores was also explored. Different printing directions led to variations in the fracture modes of the ceramic cores, as shown in Figs. 5(a) to (d). The flexural strength of the ceramic cores depends on the interlayer bonding strength of samples printed in different directions, and catastrophic fractures often occur at weak interlayer interfaces.

Mu et al.[57] prepared ceramic core green bodies using a high solid loading ceramic slurry with varying curing parameters. Figure 6 depicts a great number of interlayer gap defects along the printing direction when using a low exposure energy density and a short exposure time.

Besides the forming parameters, slurry composition also has a significant impact on the tendency for defect formation. Ozkan et al.[58] found that the slurry composition and properties had an important influence on the occurrence of crack defects during the preparation of silica-based ceramic cores. Figures 7(a) to (d) show that an excessively strong curing capability or an overly high viscosity of the slurry can lead to a heightened propensity for crack formation. Figure 7(b) shows a ceramic core prepared under optimized conditions without obvious crack defects.

The findings presented by Kong et al.[59] indicate that the utilization of the buried combustion method (BCM) can

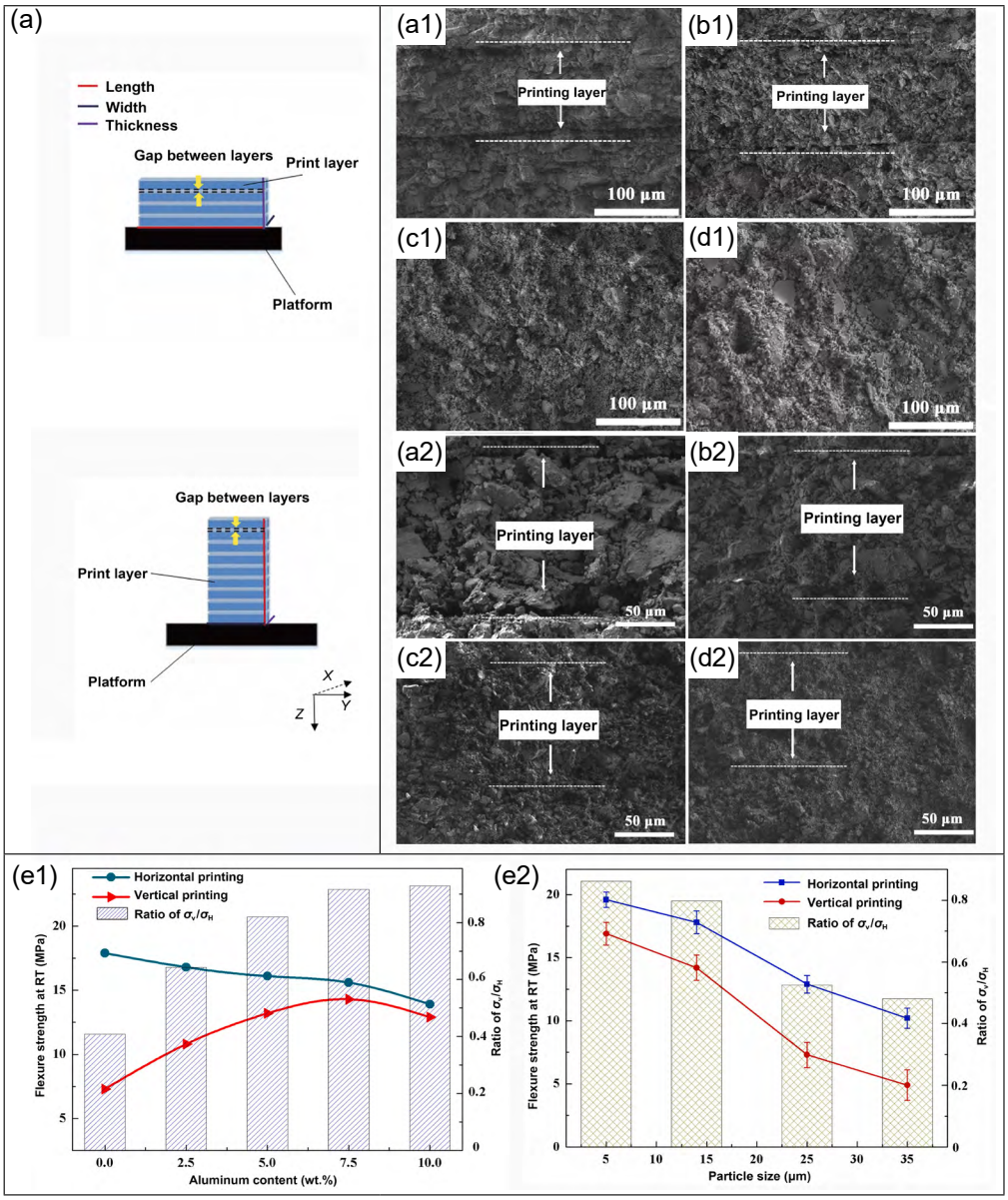

Fig. 3: Schematic diagram of different printing directions (a), microstructure of fracture surface of ceramic cores with different Al contents: (a1) 0%; (b1) 2.5%; (c1) 7.5%; (d1) 10%, and flexure strengths of ceramic cores and σ_v/σ_H ratios (e1)[51]; microstructure of fracture surface of ceramic cores with different particle sizes: (a2) 35 μm; (b2) 25 μm; (c2) 14 μm; (d2) 5 μm, and flexure strength of ceramic cores and σ_v/σ_H ratios (e2)[53]

effectively mitigate the inclination towards the generation of crack defects in alumina ceramic cores, as shown in Fig. 8(a). Further characterization revealed that buried combustion method also reduced the surface roughness of sintered ceramic cores from 2.29 μm to 0.79 μm, as illustrated in Fig. 8(b). This result proves that controlling the temperature field during debinding and sintering processes to promote orderly degradation of organic matter is an important means for suppressing crack formation. However, it is very difficult to prepare complex-structured ceramic cores through buried combustion methods. Two step debinding through atmosphere control is an effective strategy for complex structured ceramic cores[60, 61].

Hu et al.[62, 63] carried out in-depth and comprehensive research focusing on the defects associated with both structural design and the forming process of VPP 3D-printed ceramic cores. Hu et al.[62] further discovered curing error and collapse defects, as shown in Figs. 8(a1) and (b1). The principal cause of curing error lies in the insufficient stiffness of the as-cured green body. This issue is particularly pronounced when the building part incorporates thin-walled or cantilever structures. Green bodies possessing such structural configurations are prone to deformation during the printing process, ultimately leading to inaccurate printing outcomes. Collapse defects in 3D-printed ceramic cores can indeed occur due to the escalation of internal stress that occurs during the printing of thick sections within the cross-sectional structure, ultimately resulting in forming failure. In addition, they tried to design an internal lattice structure to reduce the occurrence of crack defects and believed that excessively thickness in the printed green body could increase the likelihood of crack defects during debinding, as shown in Figs. 8(a2) and (b2)[40]. Optimizing the model structure could leverage the advantages of additive

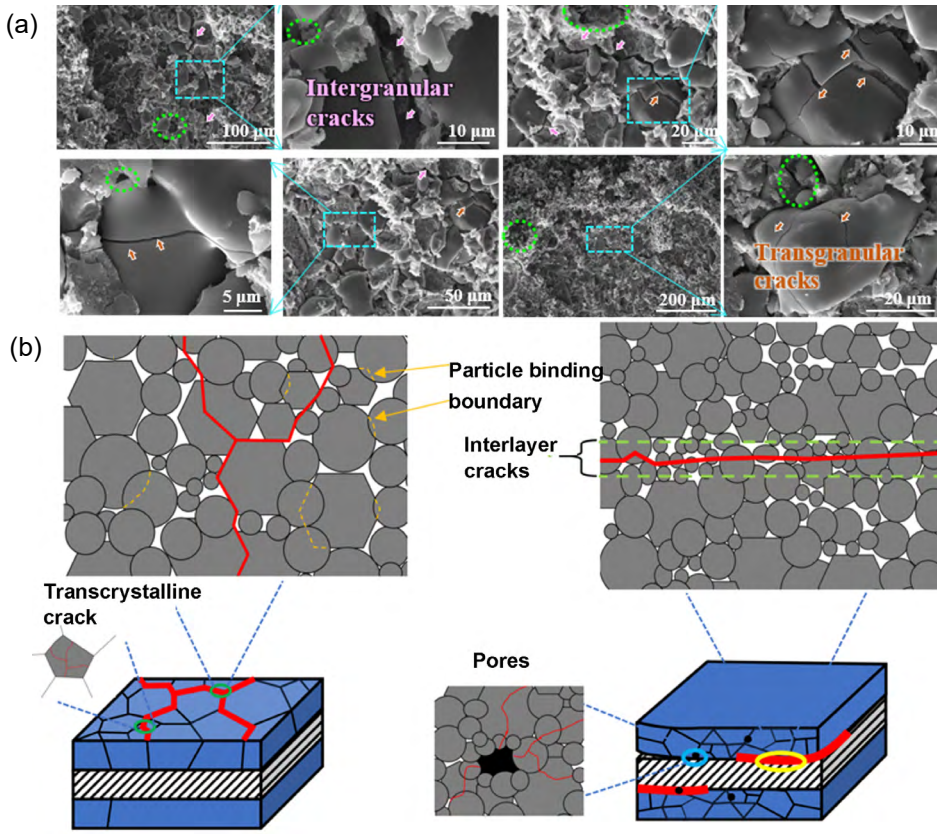

Fig. 4: SEM images of cracks in sintered ceramic cores (a) and schematic of typical microstructures at different positions within VPP 3D-printed ceramic cores (b)[55]

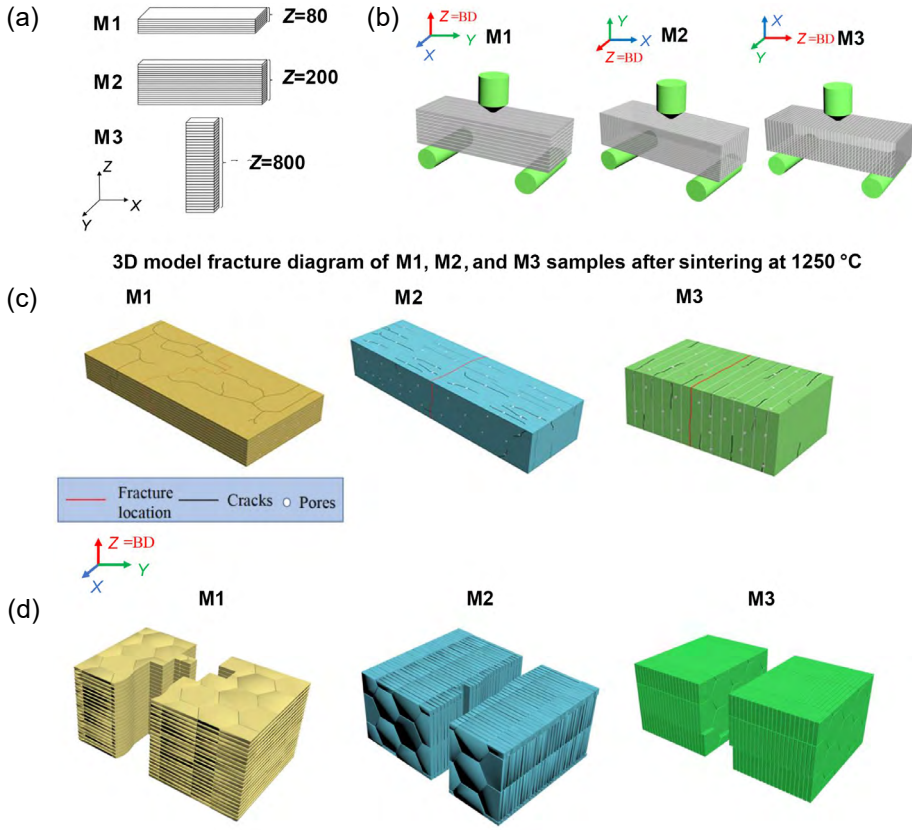

Fig. 5: Three printing models (M1–M3) of ceramic core samples (a); schematic of flexural strength test of ceramic core samples with different models (b); schematic diagram of fracture modes of ceramic cores sintered at 1,250 °C in different printing directions (M1: surface stress concentration; M2: surface stress concentration but with stronger performance; M3: weak interlayer bonding) (c); 3D fracture model of (c) (d)[56]

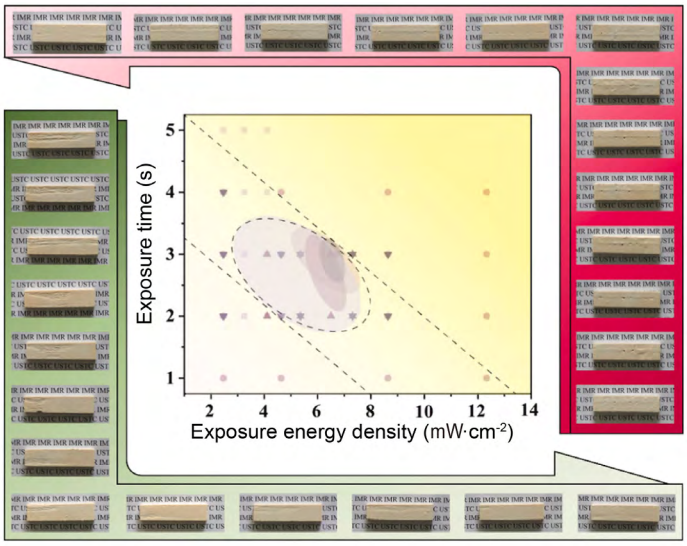

Fig. 6: Sample images of VPP 3D printed ceramic cores with different energy dose[57]

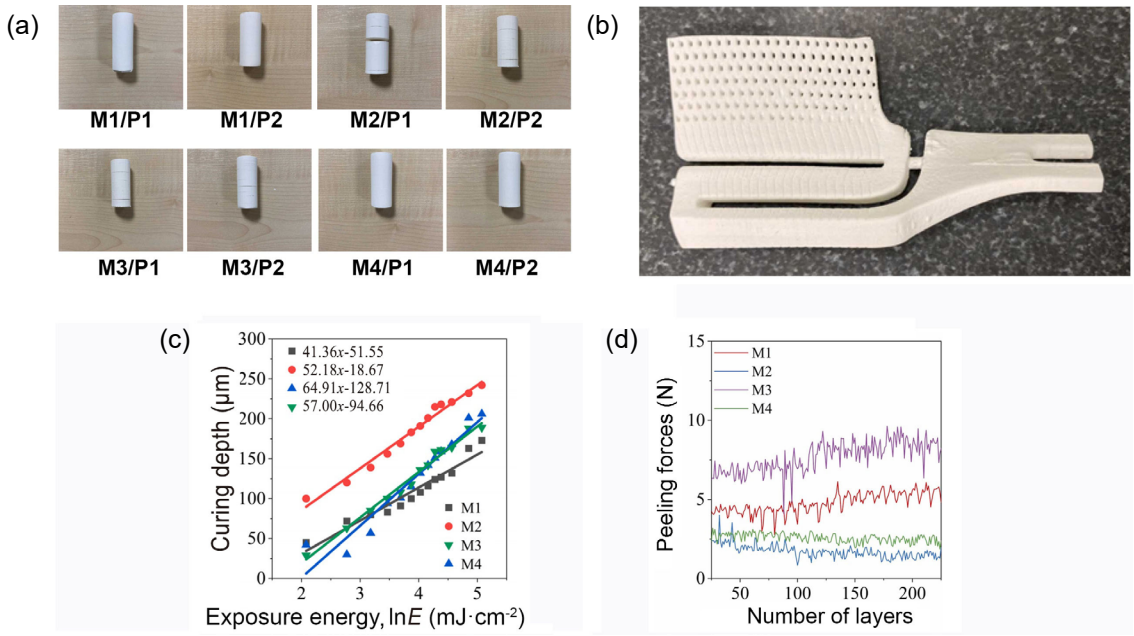

Fig. 7: Influence of binder components (M1–M4 were composed of oligomers and monomers in different ratios) and powder particle sizes (P1: d_{50}: 7.71 μm; P2: d_{50}: 12.22 μm) on layered defects: (a) condition of printed ceramic core samples; (b) a close look up of sintered ceramic core; (c) relationship between curing depth and actual energy dose; (d) peeling forces for P2 loaded suspensions, showing the impact of viscosity on peeling forces[58]

manufacturing to reduce the occurrence of crack defects. The above research results indicate that printing ceramic cores with complex structures utilizing VPP 3D method is a challenging task. Comprehensive optimization is required to suppress defects, including structural design and molding parameters.

The primary defect in ceramic cores produced by VPP 3D printing is layered crack defects caused by poor interlayer bonding[57, 61]. This defect is closely related to slurry properties, forming parameters, debinding and sintering processes. Achieving good interlayer bonding is the key to reduce layered crack defects, thus the slurry composition and forming processes have decisive influences on the layered cracks. In addition to layered cracks, sintering cracks predominantly manifest in silica-based ceramic cores, with the phase transformation of cristobalite being the primary catalyst for crack defect formation. Conversely, the predominant crystalline phase in sintered alumina-based ceramic cores is α-Al_2O_3, which does not undergo complex phase transitions that lead to cracking. Nevertheless, deformation-induced cracking during the sintering of components with intricate structures necessitates thorough investigation in both silica-based and alumina-based ceramic cores.

Apart from cracks, further defects such as curing errors and collapse occurring during the printing process also need to be studied in depth. They involve factors such as curing ability and curing shrinkage of ceramic slurry, mechanical properties of green body, and forming methods (top-down or bottom-up mode). These are the key constraints limiting the application of VPP 3D printed ceramic cores.

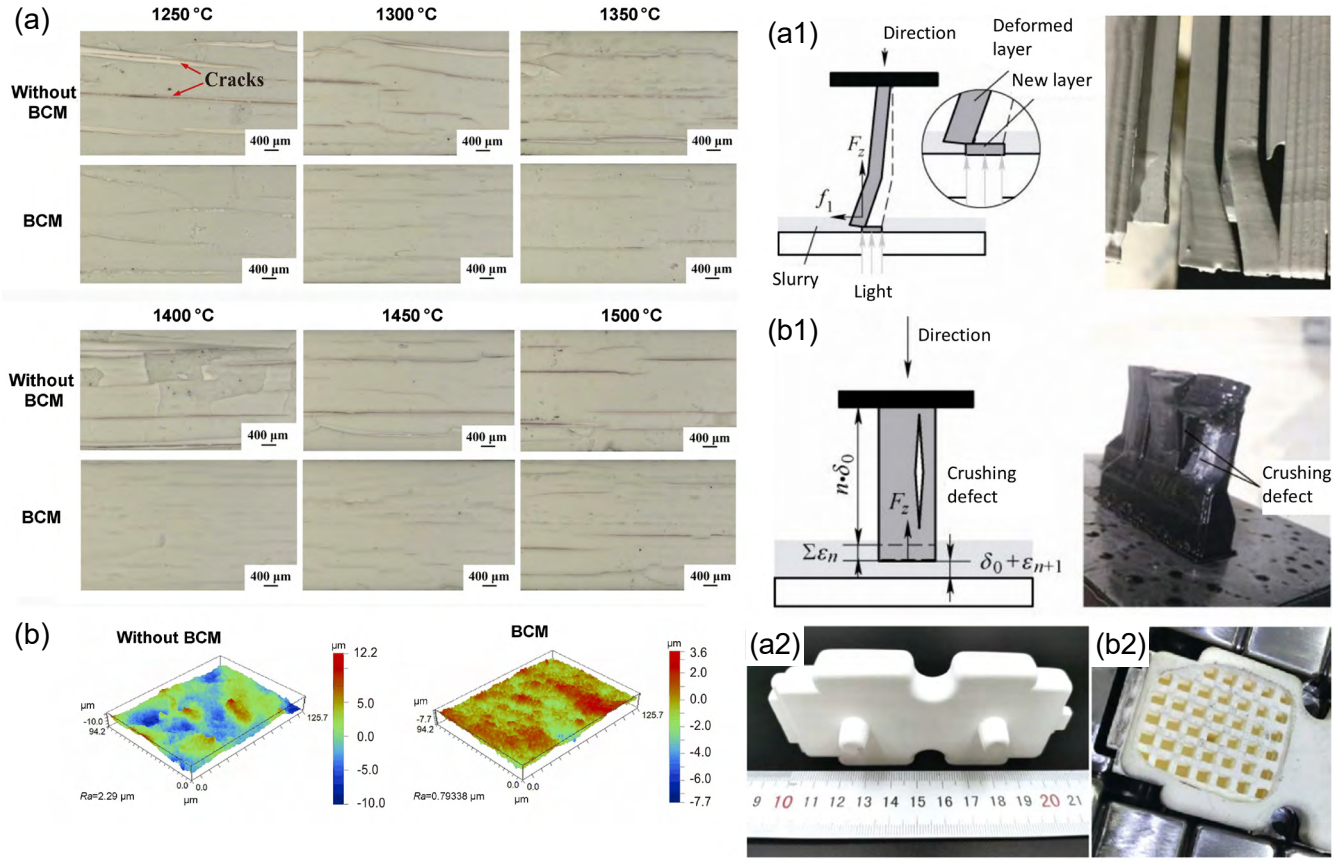

Fig. 8: Cross sections of ceramic core samples at different sintering temperatures with and without BCM (samples are directly exposed to furnace) (a), 3D surface morphology of ceramic core samples sintered at 1,300 °C with and without BCM (b)[59], schematic diagram of curing error (a1) and crushing defect (b1)[62], external surface (a2) and hollow cavity with a lattice structure (b2) of a sintered hollow core sample[40]

4 Forming accuracy and surface quality

Among various ceramic additive manufacturing technologies, VPP 3D printing boasts the highest theoretical forming precision and surface quality[64]. However, during the actual printing process, there are numerous factors that hinder the forming precision and surface quality of ceramic cores.

4.1 Forming accuracy

The slurry properties have a significant impact on forming accuracy. Ozkan et al.[65] demonstrated that the rheological behavior and curing properties of slurry were crucial factors influencing the surface quality of green bodies, as depicted in Figs. 9(a) to (e). Excessive slurry viscosity leads to higher shear forces acting on the green body during the forming process, causing deformation or damage of the green body shown in Figs. 9(f) and (g). Furthermore, the curing performance of the slurry will affect the forming quality by changing the bonding between the as-printed green body and the substrate (Only point at the equipment forming by bottom to up mode).

The forming process also has a considerable influence on printing accuracy of ceramic cores. Mu et al.[57] compared the effects of different forming parameters on accuracy, as shown in Fig. 10, and found that when the energy density is too high, the as-printed parts are prone to over-curing, which results in the loss of detailed features in the green body. Conversely, when the energy density is lower, the forming accuracy is higher. However, low energy leads to poor green body strength, making it susceptible to defects and even causing printing failures.

Doping is an important means to enhance forming accuracy. Silica-based ceramic cores use fused quartz as the main crystalline phase, which exhibits significant light scattering, thereby, reduce forming accuracy. Feng et al.[66] added an appropriate amount of graphite to the silica-based ceramic slurry to improve forming accuracy, as shown in Figs. 11(a) to (d). By increasing the absorbance of the slurry with graphite, overcuring is reduced. Additionally, hollow structures in thick sections of the ceramic cores were designed to reduce curing shrinkage and improve forming accuracy, as shown in Figs. 11(e) and (f). Niu et al.[67] incorporated mullite fibers into silica-based ceramic cores to hinder sintering shrinkage and enhance forming accuracy, as depicted in Figs. 12(a) and (b).

In addition to improving the forming accuracy, severe shrinkage during the sintering process can affect the accuracy of the final product, especially for complex-structured ceramic cores. Reducing sintering shrinkage is a crucial direction for improving the forming accuracy of ceramic cores[68]. Tang et al.[69] selected a kind of alumina powder that underwent a transformation from spherical to platelet shape during sintering to reduce the sintered shrinkage, as illustrated in Figs. 13(a) to (c). Li et al.[70]

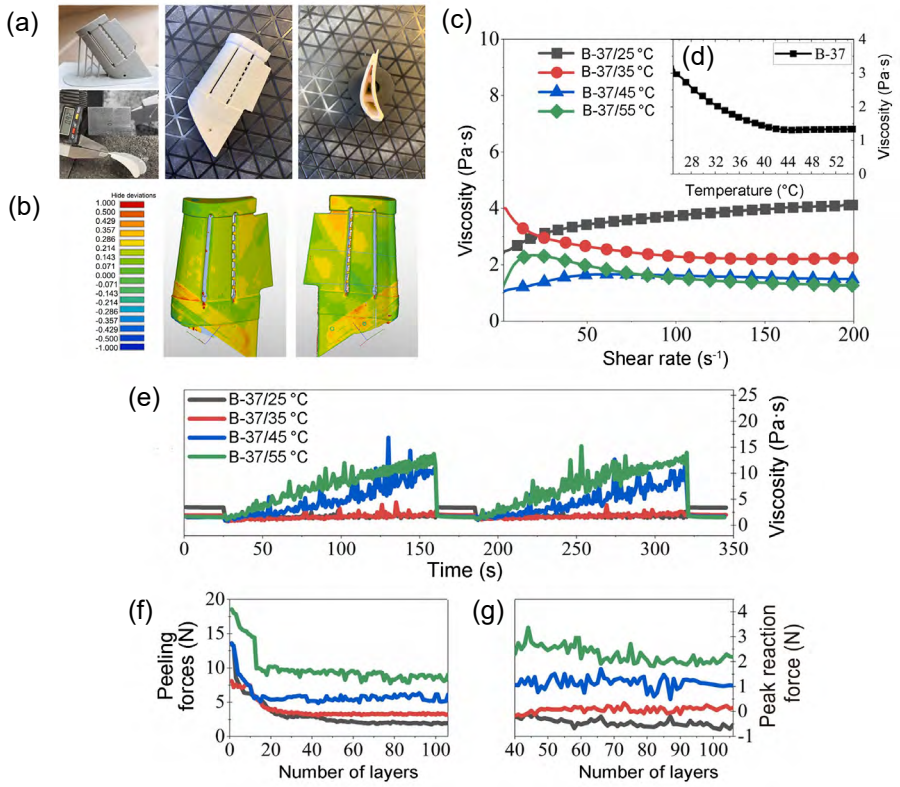

Fig. 9: Images of VPP 3D printed ceramic cores (a), precision of a sintered ceramic core fabricated by VPP 3D printing (b), rheological behavior of ceramic core slurries with the shear rate ranges from 0 to 200 s^{-1} at various temperatures (c), variation of slurry viscosity with temperature at a fixed shear rate of 100 s^{-1} (d), rheological behavior of ceramic core suspensions during different VPP printing times (e), peeling force (f) and peak reaction force (g) against number of printed layers for VPP 3D printed ceramic core samples[65]

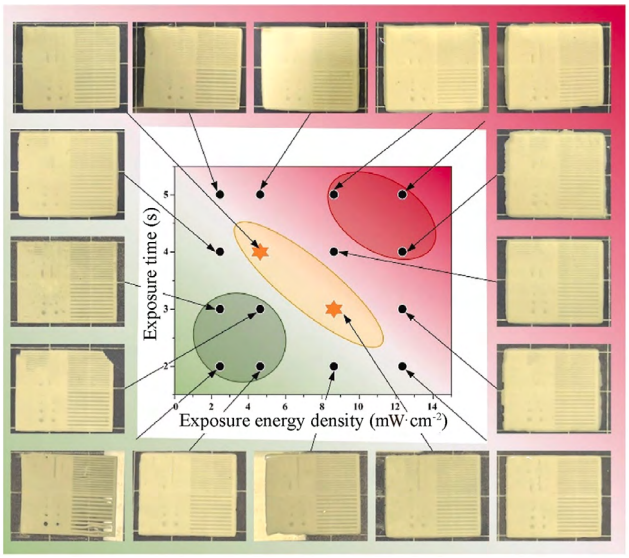

Fig. 10: Macroscopic of single-layer samples with different curing parameters[57]

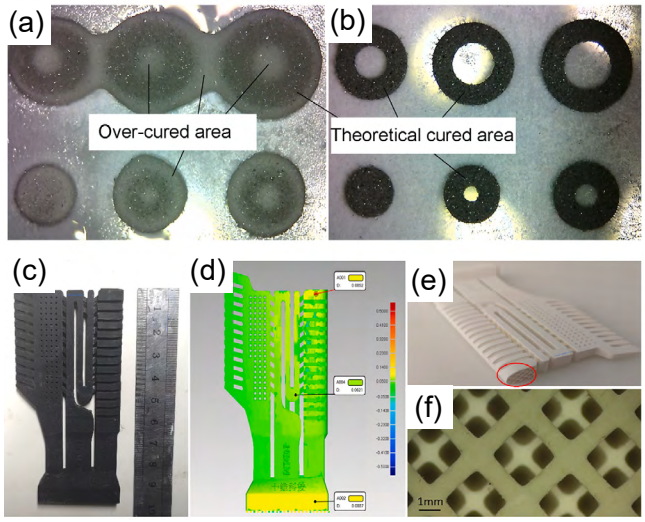

Fig. 11: Accuracy of cured samples before (a) and after (b) adding graphite to ceramic core slurries, and photos of ceramic cores with a complex structure: (c) green body; (d) forming accuracy inspection; (e) sintered ceramic core; (f) grid structure[66]

reduced the sintered shrinkage of alumina-based ceramic cores using a novel approach called atmosphere-controlled in-situ oxidation of aluminum powder, as shown in Figs. 13(a1) to (d1). Aluminum powder was protected from oxidation by argon gas at low temperatures, and the molten aluminum promoted sintering at high temperatures. After switching the atmosphere from argon to air, the molten aluminum oxidized and expanded, reducing the sintering shrinkage and improving the forming accuracy of ceramic cores.

4.2 Surface quality

Ceramic cores used for aircraft engine turbine blades require high surface quality. VPP 3D printing parameters have a significant impact on surface roughness. Xing et al.[71] analyzed the influence of layer thickness on the surface roughness of ceramic cores, as shown in Figs. 14(a) to (h). The results

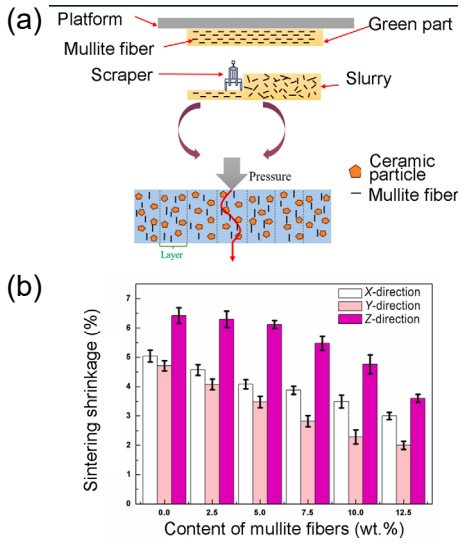

Fig. 12: Incorporation of mullite fibers into VPP 3D-printed ceramic core slurry facilitates the oriented distribution of mullite fibers (a), and sintered shrinkage of ceramic core samples in different directions versus fiber content (b)[67]

indicated that the surface roughness of the ceramic core specimens increased from *Ra*=2.3 μm to *Ra*=6.1 μm as the layer thickness increased from 25 μm to 100 μm. However, reducing the layer thickness would significantly increase the fabrication time. The layer thickness needs to be determined based on both requirements and production efficiency.

Additionally, the local angles of complex-structured ceramic cores also affect the roughness of the formed surface based on "stair-stepping effect"[73]. When the local surface curvature is larger, the stair-stepping effect on the surface becomes more obvious. This requires improving the sample placement strategy during model processing. Sintering scheme has a significant impact on the surface quality of ceramic materials.

Li et al.[72] studied the influence of sintering temperatures on the surface roughness of silica-based ceramic core specimens, as shown in Figs. 15(a) to (c). The results indicated that different sintering temperatures altered the liquid phase content, mullite formation, mullite morphology, and distribution of the amorphous phase between particles during

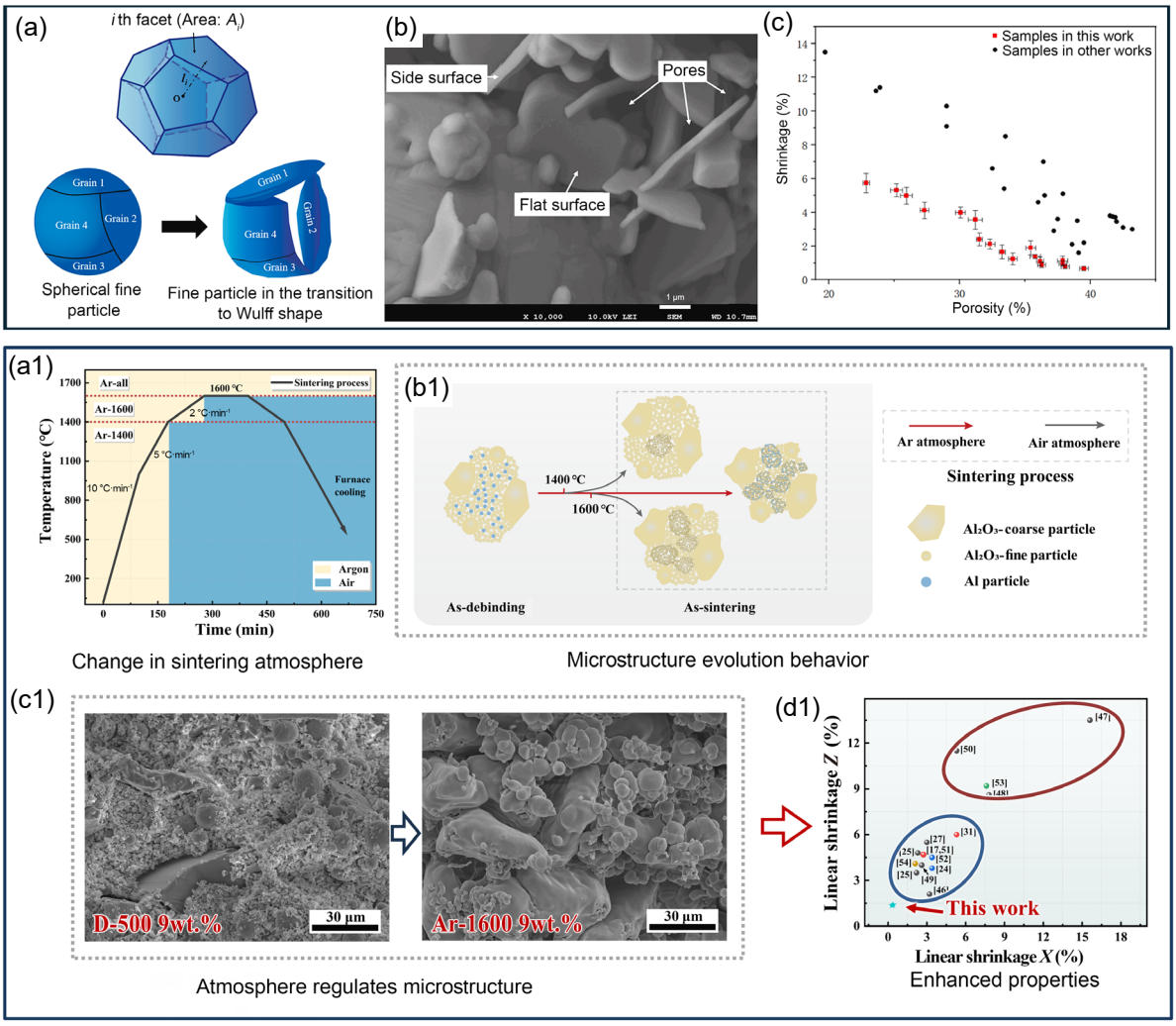

Fig. 13: Optimization of alumina ceramic core powder to reduce sintering shrinkage rate: (a) schematic diagram of the transformation of ceramic powder during sintering process; (b) microstructure of platelet-like particles within VPP 3D printed ceramic core samples; (c) comparison of shrinkage-porosity relationship between this work[69] and other works; (a1) Ar-series sintering regimes; (b1) schematic diagram of microstructure formation; (c1) microstructure change regulated by atmosphere; (d1) linear shrinkage comparison of 3D printed alumina ceramic cores[70]

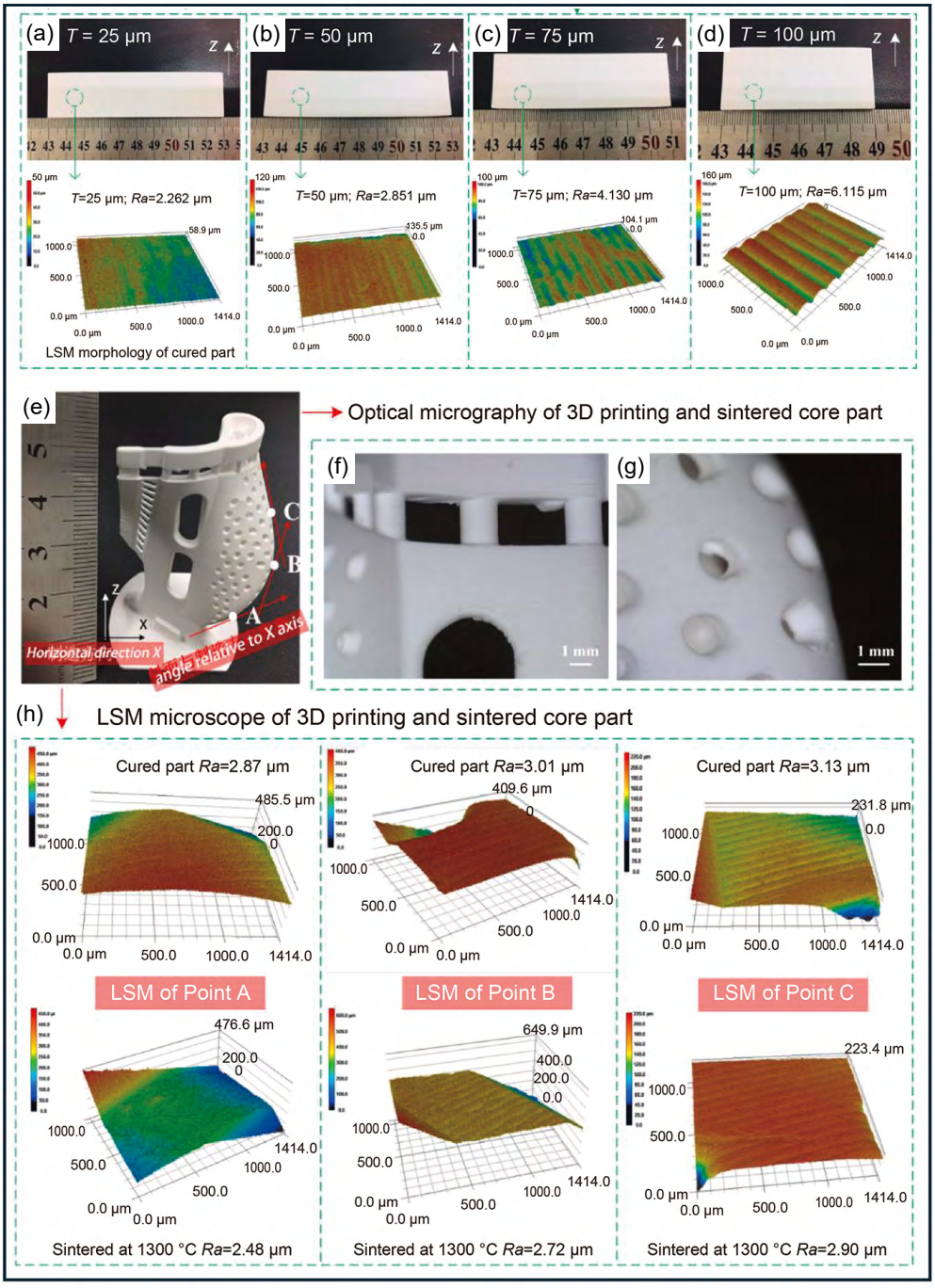

Fig. 14: Macroscopic and surface morphology of ceramic core samples with different layer thicknesses: (a) 25 μm; (b) 50 μm; (c) 75 μm; and (d) 100 μm; (e–g) micrograph of VPP 3D printed Al_2O_3 ceramic core; (h) surface morphology of different positions of green body and sintered body[71]

the sintering process of the cores. In fact, a higher degree of densification tends to result in higher surface quality. But phase transformations during sintering are often additional factors that need to be considered.

Increasing the curing depth is an effective method to improve surface quality. Li et al.[49] found that the surface roughness of the green body decreased from 2.1 μm to 1.2 μm when the curing depth was increased from 80 μm to 200 μm with a layer thickness of 50 μm. Meanwhile, the surface roughness of the sintered specimen decreased from 1.8 μm to 0.8 μm, as shown in Figs. 16(a) and (b). Furthermore, this study also showed that specimens with different printing angles exhibited different surface defects at different curing depths. A higher curing depth could significantly reduce the occurrence of surface defects. However, excessively high curing depths could easily reduce forming accuracy.

5 Challenges and prospects

Ceramic cores featuring complex geometries, high dimensional accuracy, and excellent surface finish represent a key application domain for VPP ceramic 3D printing technology. However, it has been identified that the layered structure and the lamellar defects are the first critical issues to address, particularly when

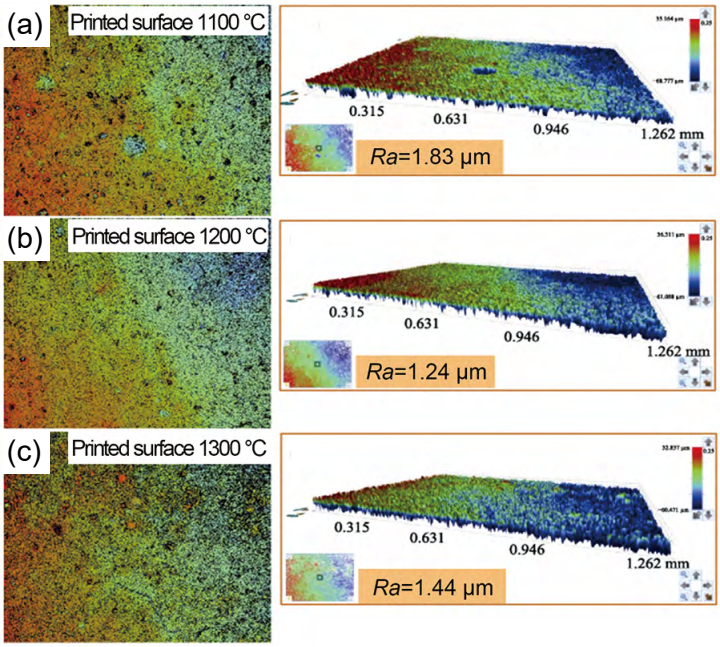

Fig. 15: 2D and 3D surface morphologies and roughness of the printed surfaces of silica-based ceramic cores sintered at different temperatures: (a1) 1,100 °C; (b1) 1,200 °C; and (c1) 1,300 °C[72]

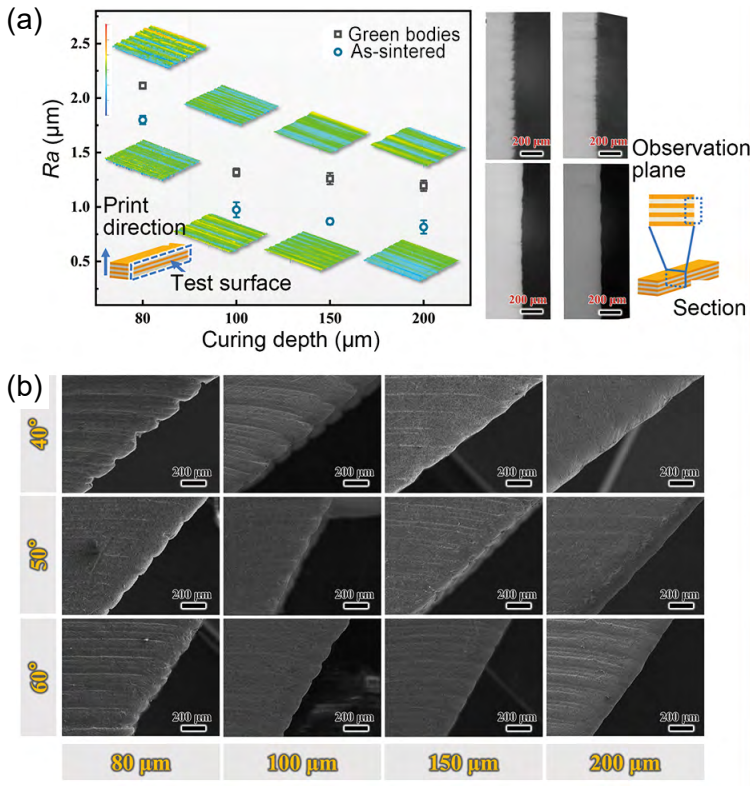

Fig. 16: Surface roughness and morphology of VPP 3D printed ceramic core green bodies and as-sintered samples (a), and SEM images of as-sintered trapezoidal samples with different bottom angles (b)[49]

fabricating samples with larger sizes or thick walls. Additionally, forming defects, such as collapse and curing error arising from slurry properties and intricate structures, constitute another key problem that needs to be resolved. When designing slurry compositions, apart from focusing on parameters like curing depth, the curing shrinkage and the strength of the green body are also crucial for achieving high-quality forming. VPP 3D printing is widely used due to its high forming accuracy and surface quality. However, the selection of powder, including crystallinity, particle size distribution, must be tailored to the specific performance requirements of the ceramic cores. This customization process, however, can introduce considerable variability, thereby compromising the accuracy of the curing mechanism. Organic composition and powder design are effective means to improve forming accuracy. However, the relevant curing theory needs further development. Finally, the sintering process often accompanies significant sintering shrinkage. Achieving near-zero sintering shrinkage is often considered an effective means to realize high-precision forming of ceramic cores with complex structures. However, near-zero sintering shrinkage places higher demands on the regulation of ceramic powders and comprehensive properties.

Acknowledgments

This work was supported by the National Key R&D Program of China (Grant Nos. 2024YFB3714502, 2024YFB3714501, 2024YFB3714504), the National Natural Science Foundation of China (Grant Nos. 52130204, 52174376), the TQ Innovation Foundation (Grant No. 23-TQ09-02-ZT-01-005), the Aeronautical Science Foundation of China (Grant No. 20220042053001), the Ningbo Science and Technology Plan Project (Grant No. 2025Z070), the Key R&D Project of Shaanxi Province (Grant Nos. 2024GX-YBXM-220, 2024CY-GJHX-29, 2024GX-ZDCYL-03-03, 2024GX-YBXM-400), the National Advanced Rare Metal Materials Innovation Center Project [Grant No. 2024 ZG-GCZX-01(1)-01], and the Foundation of China Scholarship Council (Grant No. 202406290136).

Conflict of interest

Authors declare that they have no known conflict of interest.

References

[1] Dong Y, Bu K, Dou Y, et al. Determination of interfacial heat-transfer coefficient during investment-casting process of single-crystal blades. Journal of Materials Processing Technology, 2011, 211(12): 2123–2131.
[2] Wereszczak A A, Breder K, Ferber M K, et al. Dimensional changes and creep of silica core ceramics used in investment casting of superalloys. Journal of Materials Science, 2002, 37(19): 4235–4245.

[3] Pollock T M. Alloy design for aircraft engines. Nature Materials, 2016, 15(8): 809–815.
[4] Wei Q, Zhong J, Xu Z, et al. Microstructure evolution and mechanical properties of ceramic shell moulds for investment casting of turbine blades by selective laser sintering. Ceramics International, 2018, 44(11): 12088–12097.
[5] Ren S, Bu K, Mou S, et al. Control of dimensional accuracy of hollow turbine blades during investment casting. Journal of Manufacturing Processes, 2023, 99: 548–562.
[6] Kazemi A, Faghihi-Sani M A, Nayyeri M J, et al. Effect of zircon content on chemical and mechanical behavior of silica-based ceramic cores. Ceramics International, 2014, 40(1): 1093–1098.
[7] Kazemi A, FaghihiSani M A, Alizadeh H R. Investigation on cristobalite crystallization in silica-based ceramic cores for investment casting. Journal of the European Ceramic Society, 2013, 33(15): 3397–3402.
[8] Chen Z, Li Z, Li J, et al. 3D printing of ceramics: A review. Journal of the European Ceramic Society, 2019, 39(4): 661–687.
[9] Halloran J W, Griffith M L. Ultraviolet curing of highly loaded ceramic suspensions for stereolithography of ceramics. In: Proc. Solid Freeform Fabrication, Texas: The University of Texas at Austin, 1994: 396–403.
[10] Chu T M, Szczepkowski K, Wagner W C, et al. Experimental ceramic suspensions for stereoLithography processing of implants. Journal of Dental Research, 1996, 75: 3046–3046.
[11] Brady G A, Halloran J W. Stereolithography of ceramic suspensions. Rapid Prototyping Journal, 1997, 3(2): 61–65.
[12] Mitteramskogler G, Gmeiner R, Felzmann R, et al. Light curing strategies for lithography-based additive manufacturing of customized ceramics. Additive Manufacturing, 2014, 1–4: 110–118.
[13] Oezkan B, Sameni F, Karmel S, et al. A systematic study of vat-polymerization binders with potential use in the ceramic suspension 3D printing. Additive Manufacturing, 2021, 47: 102225.
[14] Zhu N, Hou Y, Yang W, et al. Preparation of complex SiOC ceramics by a novel photocurable precursor with liquid crystal display (LCD) 3D printing technology. Journal of the European Ceramic Society, 2022, 42(7): 3204–3212.
[15] Kumar A, Dixit K, Sinha N. Fabrication and characterization of additively manufactured CNT-bioglass composite scaffolds coated with cellulose nanowhiskers for bone tissue engineering. Ceramics International, 2023, 49(11): 17639–17649.
[16] Liang C, Huang J, Wang J, et al. Three-dimensional inkjet printing and low temperature sintering of silica-based ceramics. Journal of the European Ceramic Society, 2023, 43(5): 2289–2294.
[17] Zocca A, Gomes C M, Staude A, et al. SiOC ceramics with ordered porosity by 3D-printing of a preceramic polymer. Journal of Materials Research, 2013, 28(17): 2243–2252.
[18] Minas C, Carnelli D, Tervoort E, et al. 3D printing of emulsions and foams into hierarchical porous ceramics. Advanced Materials, 2016, 28(45): 9993–9999.
[19] Du W, Ren X, Ma C, et al. Ceramic binder jetting additive manufacturing: Particle coating for increasing powder sinterability and part strength. Materials Letters, 2019, 234: 327–330.
[20] Sahu K K, Modi Y K. Multi response optimization for compressive strength, porosity and dimensional accuracy of binder jetting 3D printed ceramic bone scaffolds. Ceramics International, 2022, 48(18): 26772–26783.
[21] Tang H H, Chiu M L, Yen H C. Slurry-based selective laser sintering of polymer-coated ceramic powders to fabricate high strength alumina parts. Journal of the European Ceramic Society, 2011, 31(8): 1383–1388.
[22] Chen A N, Li M, Xu J, et al. High-porosity mullite ceramic foams prepared by selective laser sintering using fly ash hollow spheres as raw materials. Journal of the European Ceramic Society, 2018, 38(13): 4553–4559.
[23] Shishkovsky I, Yadroitsev I, Bertrand P, et al. Alumina-zirconium ceramics synthesis by selective laser sintering/melting. Applied Surface Science, 2007, 254(4): 966–970.
[24] Wilkes J, Hagedorn Y C, Meiners W, et al. Additive manufacturing of ZrO_2-Al_2O_3 ceramic components by selective laser melting. Rapid Prototyping Journal, 2013, 19(1): 51–57.
[25] Hafkamp T, van Baars G, de Jager B, et al. A feasibility study on process monitoring and control in vat photopolymerization of ceramics. Mechatronics, 2018, 56: 220–241.
[26] Liu Y, Chen Z W. Research progress in photopolymerization-based 3D printing technology of ceramics. Journal of Materials Engineering, 2020, 48(9): 1–12.
[27] Zakeri S, Vippola M, Levänen E. A comprehensive review of the photopolymerization of ceramic resins used in stereolithography. Additive Manufacturing, 2020, 35: 101177.
[28] Yu X, Niu Y, Jiang W, et al. Significantly improved sintering shrinkage of heavy calcium carbonate ceramic cores by binder jetting using Al powder additive. Ceramics International, 2024, 50(21): 40922–40931.
[29] Zhao W, Liu W, Chang J, et al. Properties comparison of pure Al_2O_3 and doped Al_2O_3 ceramic cores fabricated by binder jetting additive manufacturing. Ceramics International, 2023, 49(24): 40336–40346.
[30] Mu Y, Liu F, Zhang C, et al. Fabrication of high-strength and anti-hydration water-soluble calcia-based ceramic core modified with nano-ZrO_2 via direct ink writing method. Ceramics International, 2023, 49(23): 38623–38634.
[31] Zhang J, Wu J M, Liu H, et al. Infiltration of silica slurry into silica-based ceramic cores prepared by selective laser sintering based on pre-sintering. Ceramics International, 2023, 49(19): 31477–31484.
[32] Zheng W, Wu J, Chen S, et al. Fabrication of high-performance silica-based ceramic cores through selective laser sintering combined with vacuum infiltration. Additive Manufacturing, 2021, 48: 102396.
[33] Kim E H, Choi H H, Jung Y G. Fabrication of a ceramic core for an impeller blade using a 3D printing technique and inorganic binder. Journal of Manufacturing Processes, 2020, 53: 43–47.
[34] Halloran J W. Ceramic stereolithography: Additive manufacturing for ceramics by photopolymerization. Annual Review of Materials Research, 2016, 46(1): 19–40.
[35] Maristany E, Cordero Z C, Boyer J, et al. Economics of 3D printing ceramic cores for gas turbine investment castings. Additive Manufacturing Letters, 2024, 10: 100223.
[36] Wang Y, Bu Y, Wang X. Advances in 3D printing of structural and functional ceramics: Technologies, properties, and applications. Journal of the European Ceramic Society, 2024, 44(14): 116653.
[37] Li W, Zhou H, Liu W, et al. Research progress in ceramic slurries and rheology via photopolymerization based 3D printing. Journal of Materials Engineering, 2022, 50(7): 40–50.
[38] Guo Z, Song Z, Fan J, et al. Experimental and analytical investigation on service life of film cooling structure for single crystal turbine blade. International Journal of Fatigue, 2021, 150: 106318.
[39] Li J, An X, Liang J, et al. Recent advances in the stereolithographic three-dimensional printing of ceramic cores: Challenges and prospects. Journal of Materials Science & Technology, 2022, 117: 79–98.
[40] Hu K, Wang H, Lu K, et al. Fabrication of silica-based ceramic cores with internal lattice structures by stereolithography. China Foundry, 2022, 19(5): 369–379.
[41] Wang Q, Wang C, Lu Z, et al. Performance of silicon oxide-based ceramic cores made by rapid prototyping for single crystal turbine blades. Journal of Materials Engineering, 2022, 50(7): 51–58. (In Chinese)

[42] Wang C, Yang Z, Ma H. Application of numerical simulation in ceramic powders pressing process. Journal of Synthetic Crystals, 2007, 36(2): 415–418, 423.
[43] Zhao D, Su H, Hu K, et al. Formation mechanism and controlling strategy of lamellar structure in 3D printed alumina ceramics by digital light processing. Additive Manufacturing, 2022, 52: 102650.
[44] Li Q, Hou W, Liang J, et al. Controlling the anisotropy behaviour of 3D printed ceramic cores: From intralayer particle distribution to interlayer pore evolution. Additive Manufacturing, 2022, 58: 103055.
[45] Li Q, Qiu Y, Hou W, et al. Slurry flow characteristics control of 3D printed ceramic core layered structure: Experiment and simulation. Journal of Materials Science & Technology, 2023, 164(20): 215–228.
[46] Park H, Yeo J, Choi J, et al. Ceramic green and fired body with a uniform microstructure prepared using living characteristics of photo-curable cycloaliphatic epoxide: Applicability of cycloaliphatic epoxide in photo-polymerization-based 3D printing. Journal of the European Ceramic Society, 2022, 42(2): 589–599.
[47] Chartier T, Dupas C, Geffroy P, et al. Influence of irradiation parameters on the polymerization of ceramic reactive suspensions for stereolithography. Journal of the European Ceramic Society, 2017, 37(15): 4431–4436.
[48] Li X, Hu K, Lu Z. Effect of light attenuation on polymerization of ceramic suspensions for stereolithography. Journal of the European Ceramic Society, 2019, 39(7): 2503–2509.
[49] Li X, Su H, Dong D, et al. Selection strategy of curing depth for vat photopolymerization 3D printing of Al_2O_3 ceramics. Additive Manufacturing, 2024, 88: 104240.
[50] Niu S, Luo Y, Li X, et al. 3D printing of silica-based ceramic cores reinforced by alumina with controlled anisotropy. Journal of Alloys and Compounds, 2022, 922: 166325.
[51] Li X, Liu Z, Niu S, et al. Controlled anisotropy in 3D printing of silica-based ceramic cores through oxidization reaction of aluminum powders. Ceramics International, 2023, 49(15): 24861–24867.
[52] Li J, Niu S, Li X, et al. Inter-layer structures regulated by metallic Si powders in 3D printing of silica-based ceramic cores. Ceramics International, 2024, 50(13): 23389–23399.
[53] Fan J, Xu X, Niu S, et al. Anisotropy management on microstructure and mechanical property in 3D printing of silica-based ceramic cores. Journal of the European Ceramic Society, 2022, 42(10): 4388–4395.
[54] Sun Y, Qian C, Hu K, et al. Cellular automata simulation of interlayer microstructure for alumina ceramic sintering process formed by vat photopolymerization. Journal of the European Ceramic Society, 2023, 44(4): 2280–2293.
[55] An X, Chen J, Mu Y, et al. Crack initiation and propagation in a high-solid-loading ceramic core fabricated through stereolithography 3D printing. Open Ceramics, 2022, 11: 100295.
[56] An X L, Liang J J, Li J G, et al. Sample selection for models to represent ceramic cores fabricated by stereolithography three-dimensional printing. Journal of Materials Science & Technology, 2022, 121: 117–123.
[57] Mu Y, Chen J, An X, et al. Defect control in digital light processing of high-solid-loading ceramic core. Ceramics International, 2022, 48(19): 28739–28744.
[58] Ozkan B, Sameni F, Karmel S, et al. Binder stabilization and rheology optimization for vat-photopolymerization 3D printing of silica-based ceramic mixtures. Journal of the European Ceramic Society, 2022, 43(4): 1649–1662.
[59] Kong D, Guo A, Hu Y, et al. Alumina-based ceramic cores prepared by vat photopolymerization and buried combustion method. Materials Today Communications, 2023, 37: 107434.
[60] Liu K, Sun Y, Sun H, et al. Effect of particle grading on the properties of photosensitive slurry and $BaTiO_3$ piezoelectric ceramic via digital light processing 3D printing. Journal of the European Ceramic Society, 2023, 43(8): 3266–3274.
[61] Zhou M, Liu W, Wu H, et al. Preparation of a defect-free alumina cutting tool via additive manufacturing based on stereolithography – Optimization of the drying and debinding processes. Ceramics International, 2016, 42(10): 11598–11602.
[62] Hu K, Lu Z, Lu K, et al. Additive manufacturing of complex ceramic cores and verification of casting process. Journal of Mechanical Engineering, 2021, 57(3): 227–234.
[63] Hu K, Wei Y, Lu Z, et al. Design of a shaping system for stereolithography with high solid loading ceramic suspensions. 3D Printing and Additive Manufacturing, 2018, 5(4): 311–318.
[64] Zhang X, Zhang K, Zhang L, et al. Additive manufacturing of cellular ceramic structures: From structure to structure-function integration. Materials & Design, 2022, 215: 110470.
[65] Ozkan B, Sameni F, Goulas A, et al. Hot ceramic lithography of silica-based ceramic cores: The effect of process temperature on vat-photopolymierisation. Additive Manufacturing, 2022, 58: 103033.
[66] Feng Q, Hu K, Wang H, et al. Forming deviation coupling model and control method in the photopolymerization process of ceramic slurry. Ceramics International, 2023, 50(5): 8490–8499.
[67] Niu S, Wang K, Luo Y, et al. Enhanced high-temperature dimensional accuracy by fibers in silica ceramic cores prepared through vat photopolymerization 3D printing. Ceramics International, 2024, 50(14): 25886–25894.
[68] Qin Y, Pan W. Effect of silica sol on the properties of alumina-based ceramic core composites. Materials Science and Engineering: A, 2009, 508(1): 71–75.
[69] Tang W, Zhao T, Dou R, et al. Additive manufacturing of low-shrinkage alumina cores for single-crystal nickel-based superalloy turbine blade casting. Ceramics International, 2022, 48(11): 15218–15226.
[70] Li X, Su H, Dong D, et al. New approach to preparing near zero shrinkage alumina ceramic cores with excellent properties by vat photopolymerization. Journal of Materials Science & Technology, 2024, 193: 61–72.
[71] Xing H, Lai L, Zhao Y, et al. Coating optimization of yield pseudoplastic paste-based stereolithography 3D printing of alumina ceramic core. Ceramics International, 2022, 48(20): 30118–30126.
[72] Li Q, Gu Y, Yu X, et al. Effect of sintering temperature on surface morphology and roughness of 3D-printed silicon ceramic cores. Journal of Inorganic Materials, 2022, 37(3): 325–332.
[73] Wang X, Zhou Y, Zhou L, et al. Microstructure and properties evolution of silicon-based ceramic cores fabricated by 3D printing with stair-stepping effect control. Journal of the European Ceramic Society, 2021, 41(8): 4650–4657.